

Intracellular Pathway Followed by the Insulin Receptor Covalently Coupled to ^{125}I -Photoreactive Insulin during Internalization and Recycling

Jean-Louis Carpentier,* H el ene Gazzano,† Emmanuel Van Obberghen,† Max Fehlmann,† Pierre Freychet,† and Lelio Orci*

*Institute of Histology and Embryology, University of Geneva Medical School, 1211 Geneva 4, Switzerland; †Institut National de la Sant e et de la Recherche M edicale, (INSERM U 145) Facult e de M edicine, Nice, France

Abstract. After it interacts with a specific receptor on the cell surface, insulin is internalized in its target cell by an adsorptive endocytotic process and eventually degraded in lysosomes. It was also recently shown that the initial surface interaction between the hormone and its receptor is followed by an internalization of the receptor, which later is recycled back to the cell surface.

In the present study the insulin receptor was tagged with a ^{125}I -photoreactive insulin analogue that can be covalently coupled to the insulin receptor by ultraviolet

irradiation. Using this tool we could trace by quantitative electron microscope autoradiography the intracellular pathway followed by this labeled receptor. The quantitative analysis of the intracellular distribution of the labeled material as a function of incubation time at 37°C supports the following sequence of events: association first with clear vesicles, second with multivesicular bodies, third with dense bodies, and fourth, a return to the cell surface via clear vesicles. This insulin receptor recycling process is inhibited by monensin but unaffected by cycloheximide.

THE concept of recycling of plasma membrane components was first postulated on kinetic grounds. Steinman et al. observed that the rapid turnover rate of the plasma membrane proteins of L cells required the recycling of membrane components since it was more rapid than could be explained by protein synthesis (39). Later, the occurrence of a recycling process for membrane receptors (which represent highly specialized structural units in the membrane) was inferred from studies of various receptors, i.e., for asialoglycoproteins, LDL, transferrin, mannose-6-phosphate, mannose, α_2 -macroglobulin, and chemotactic peptide receptor (1, 2, 11, 20, 22, 24, 25, 35, 37, 38, 41, 42, 46). Based on these observations, various studies were designed to trace the pathway followed by receptors on their way to and from the cell surface. The results of these analyses converged to demonstrate that most receptor–ligand complexes accumulate in coated pits on the plasma membrane, are internalized through coated vesicles, and later associate with an intermediary storage vacuole, the endosome (5, 23, 30, 40). This organelle seems to be an important sorting center where the ligand and its receptor can be uncoupled before being marshalled in separate directions: usually, lysosomes for the ligand and the cell surface for recycling receptors (5, 12, 19, 23, 30, 40, 42, 43). At present however, although the fate of the ligands has been extensively characterized, limited morphological information is available about the organelles that are involved in the recycling of receptors back to the cell surface (19, 22).

Recently, the use of a photoreactive ^{125}I -insulin analogue

allowed us to tag the insulin receptor and to follow its internalization and recycling both biochemically and morphologically (15, 16, 21). In the present study we took advantage of this remarkable tool to define by quantitative electron microscope (EM)¹ autoradiography the structures involved in this journey of the receptor inside the cell. Results obtained suggest that the slow recycling process observed using ^{125}I -photoreactive insulin covalently coupled to the insulin receptors is occurring through the lysosomal compartment via a population of clear vesicles.

Materials and Methods

Photoreactive Insulin

The photoreactive insulin analogue [2-nitro-4-azidophenylacetyl (B2)] des-Phe-B1-insulin was prepared as previously described (17). This analogue retains 70% of the receptor binding affinity and the biological potency of native insulin (17). The photoreactive insulin was iodinated in the dark to a specific activity of 200–250 $\mu\text{Ci}/\mu\text{g}$ by using the same method as that described for native insulin (18).

Insulin Binding Studies

Hepatocytes were isolated from male Wistar rats (120–150 g) by collagenase dissociation by a modification of the method described by Seglen (36). Immediately after their isolation, hepatocytes (0.5×10^6 cells per ml) were incubated in the dark in Krebs-Ringer bicarbonate (KRb) buffer (pH 7.4) containing 10 mg/ml bovine serum albumin, gentamycin at 50 $\mu\text{g}/\text{ml}$, bacitracin at 0.8 mg/ml, and 2 mM phenylmethylsulfonyl fluoride (PMSF) with ^{125}I -labeled photo-

¹ Abbreviations used in this paper: EM, electron microscope; KRb, Krebs-Ringer bicarbonate; UV, ultraviolet.

reactive insulin for 2 h at 15°C, a condition in which steady state binding with minimal insulin internalization is attained (8). At the end of the association step, isolated hepatocytes were collected by centrifugation and resuspended in the same volume of insulin-free buffer at 4°C. Cells were then exposed to ultraviolet (UV) light as detailed below. Hepatocytes were then diluted 20-fold in insulin-free buffer and thereafter incubated for up to 6 h at 37°C. When indicated monensin (10^{-6} M) (Calbiochem-Behring Corp., San Diego, CA), or cycloheximide (10^{-4} M) (Sigma Chemical Co., St. Louis, MO) was present throughout the 37°C incubation. Nonspecific binding was determined in simultaneous experiments in which unlabeled insulin (5 μ M) was added to the incubation at the beginning of the association period.

Irradiation Procedure Used for Covalent Affinity Labeling of Insulin Receptors

All irradiation was conducted, under standardized conditions, in a cold room (4°C) using a water-cooled high pressure mercury lamp (Philips HPK 125 W). The light was filtered through a "black glass" filter (UV W. 55, Hanau, FRG). Suspensions (3 mm depth) of freshly isolated hepatocytes were irradiated for 3 min at 9 cm from the lamp. By using this irradiation procedure the hepatocytes retained both morphological integrity and biological responsiveness to insulin (16, 17).

Analysis of Cell-associated Radioactivity

In a separate set of incubations at 37°C after UV irradiation, isolated hepatocytes were centrifuged and washed as described above. The washed pellet was then extracted with a mixture of 0.1% Triton X-100 (Rohm and Haas Co., Philadelphia, PA), 3 M acetic acid and 6 M urea. The mixture was centrifuged in a Beckman microfuge at 12,000 *g* for 5 min at room temperature, and 95–98% of the total cellular radioactivity was found in the supernate. The supernate was applied to a Sephadex G-50 Fine column (0.9 × 50 cm), which was equilibrated and eluted in the extraction mixture. 1-ml samples were collected on an automated fraction collector.

Preparation of Cells for Electron Microscopy and Autoradiography

At each time point an aliquot of the cell suspension was washed in KRb buffer and fixed for a minimum of 2 h with 2% glutaraldehyde in 0.1 M phosphate buffer (pH 7.4) for electron microscopic analysis. The fixed sample was processed for electron microscopic autoradiography as previously described (9, 10).

Sampling and Analysis of the Data

The method of sampling was similar to that described previously (9, 10). Three different incubations were carried out for each experimental condition. For each time point in each experiment ~200 grains were photographed. Since three experiments were performed, ~600 grains were analyzed per time point. All determinations were carried out on positive prints enlarged three times (final magnification, 42,000).

The association of the labeled material with the plasma membrane of the hepatocyte was assessed quantitatively by the method of Salpeter et al. (31). By the use of this method the percentage of total number of grains was plotted as a function of the distance between the grain center and the closest plasma membrane, as previously described (9).

The relationship of autoradiographic grains to plasma membrane and intracellular structures was assessed by the "hypothetical grains" method of Blackett and Parry (4). 12 different structures were chosen as potential sources of radioactivity in the hypothetical grains analysis, and 19 structural subdivisions were made for the location of both observed and hypothetical grains. Due to small differences in the time courses of 125 I-photoreactive insulin internalization and recycling from one experiment to the other, results from each experiment had to be analyzed separately and could not be pooled. In consequence, the number of grains photographed in each experiment limited the application of the "hypothetical grains" method to the localization of the labeled material and was not accurate enough to allow a quantitative evaluation of the labeling pattern as a function of time. Knowing which structures were labeled, we determined the percentage of grains associated with these structures under the various experimental conditions tested. Grains overlying the cytoplasm (>250 nm from the plasma membrane) were divided into the following classes based on their relation to the following structures: clear vesicles; lysosomes (dense bodies); multivesicular bodies; Golgi complexes; shared association clear vesicles/dense bodies; shared association clear vesicles/multivesicular bodies; other structures. Grains were categorized in one of these groups when a 250-nm-

diam circle superposed over the grain included part or all of the corresponding structure or group of structures. After 2 h of incubation at 15°C the number of grains associated with the cytoplasm was low; therefore the three different experiments were pooled to reach a satisfactory number of pictures for the quantitative analysis.

The volume densities of clear vesicles, multivesicular bodies, and dense bodies were determined under two different incubation conditions: 0 and 300 min of incubation at 37°C after UV irradiation. For each condition 43 to 57 randomly taken pictures were analyzed from three different Epon blocks. Morphometric determination was made on prints enlarged three times (final magnification, 42,000) with a test screen (160 × 205 mm) in the form of a double period square lattice (with a 1:9 ratio) according to Weibel (44) as previously described (10).

To measure the size of clear vesicles and multivesicular bodies, the shape of these organelles was approximated by circles and the diameter of the circles was determined by comparison with calibrated circles.

Results

General Characteristics of the Hepatocytes

The isolated hepatocytes used for these experiments have the typical morphological characteristics of isolated hepatocytes previously used and described (10, 16). Up to 5 h of incubation at 37°C after UV irradiation, the proportion of damaged cells remained constant (<25%). In contrast, after 5 h at 37°C the morphological study showed an increased proportion of necrotic hepatocytes.

The cytoplasm of cells incubated in the presence of monensin (10^{-6} M) showed a dilation of the Golgi cisternae and of vacuoles with dispersed electron dense material, together with an enlargement of multivesicular bodies (Figs. 1 and 2). Up to 3 h of incubation at 37°C in the presence of monensin, the proportion of necrotic cells remained constant (<25%), but after longer incubations the proportion of necrotic cells increased, excluding any morphological analysis of these time points. Cycloheximide (10^{-4} M) had no visible effect on the cell morphology.

Nature of the Cell-associated Radioactivity

At the end of various incubation periods at 37°C, the cell-associated radioactivity was extracted in a mixture of Triton X-100, urea, and acetic acid. Under these conditions, 95–98% of the cell-associated radioactivity was recuperated and either applied to a Sephadex G-50 column or analyzed by SDS PAGE. When layered on a Sephadex G-50 column, most of the radioactivity was recovered in two peaks: one eluting in the position of 125 I-insulin (125 I-photoreactive insulin) and the other eluting in a region of higher molecular weight molecules corresponding to 125 I-photoreactive insulin-receptor complexes (as demonstrated by SDS PAGE [15, 16]). After 2 h of incubation at 15°C in the presence of 125 I-photoreactive insulin, the amount of radioactivity associated with these two peaks was in the proportion 2:3 125 I-photoreactive insulin, 1:3 125 I-photoreactive insulin-receptor complexes. As a function of incubation time at 37°C, the amount of radioactivity recovered in the form of 125 I-photoreactive insulin-receptor complexes remained practically constant as shown not only by Sephadex G-50 chromatography (Fig. 3) but also by SDS PAGE (Fig. 2B in reference 15). In contrast, the radioactivity eluting in the region of 125 I-insulin dropped continuously so that by 60 min the two radioactive peaks were in the proportion 2:3 125 I-photoreactive insulin-receptor complexes, 1:3 125 I-photoreactive insulin (Fig. 3). After longer incubations, the decrease in cell-associated radioactivity observed between 1 and 2 h of incubation at 37°C (Fig. 4 in

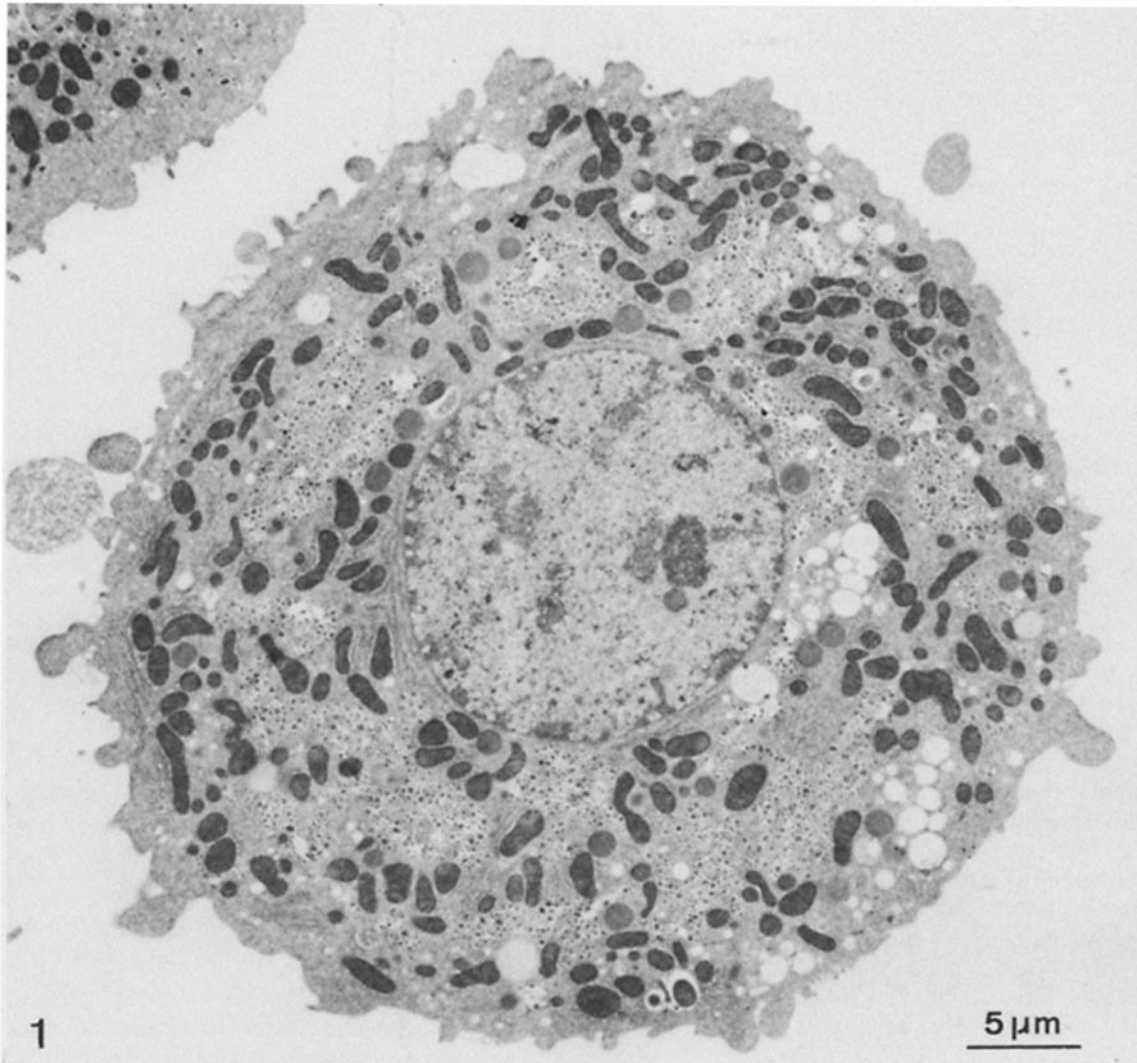


Figure 1. Low magnification view of an isolated hepatocyte incubated for 2 h at 15°C in the presence of ^{125}I -photoreactive insulin, UV irradiated, washed, resuspended for 30 min at 37°C in incubation buffer in the presence of 10^{-6} M monensin, and processed for EM autoradiography.

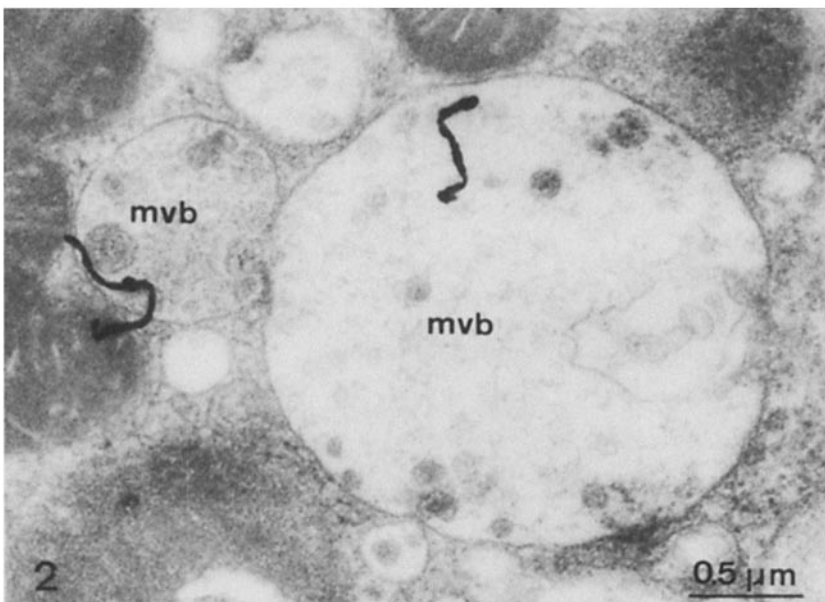


Figure 2. View of a portion of cytoplasm of an isolated hepatocyte incubated for 2 h at 15°C in the presence of ^{125}I -photoreactive insulin, UV irradiated, washed, and resuspended for 180 min at 37°C in incubation buffer in the absence of any labeled insulin. 10^{-6} M monensin was present during the 37°C incubation. Autoradiographic grains are seen in the vicinity of the limiting membrane of multivesicular bodies (mvb).

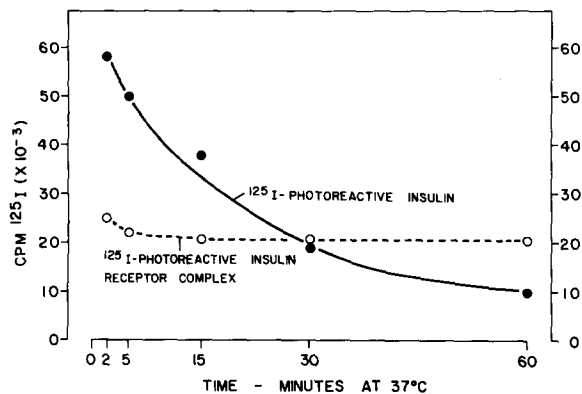


Figure 3. Nature of the hepatocyte-associated radioactivity at various incubation times at 37°C. At appropriate incubation times, cells were separated from the incubation media by centrifugation and washed with buffer. The cell pellet was extracted with a mixture of 0.1% Triton X-100, 4 M acetic acid, and 6 M urea, resulting in the extraction of 95–98% of the total radioactivity. The extract was then applied to a G-50 Sephadex column developed in and eluted by the extracting solvent. Most of the cell-associated radioactivity was recovered in two peaks: one eluting in the position of ^{125}I -insulin, and the other eluting in a region of higher molecular weight molecules and corresponding to the ^{125}I -photoreactive insulin receptor complexes. The amount of radioactivity associated with these two peaks at the various incubation times at 37°C was recorded.

reference 15) was accounted for by a further decrease in cell-bound ^{125}I -photoreactive insulin, since the amount of radioactivity recovered in ^{125}I -photoreactive insulin–receptor complexes remained constant at these incubation times (Fig. 2B in reference 15). Taken together, these biochemical data indicate that at least by 60 min of incubation at 37°C, and after longer incubations, most of the cell-associated radioactivity available for quantitative EM autoradiography corresponds to ^{125}I -photoreactive insulin–receptor complexes.

Association of Radioactivity with the Plasma Membrane as a Function of Time

During the 15°C association period, autoradiographic grains were predominantly associated with the plasma membrane of isolated hepatocytes: at the end of the 2-h incubation only 5–10% of the cell-associated radioactivity was internalized² (Figs. 4 and 6B). Similar to previous observations carried out with ^{125}I -insulin (8), a progressive concentration of ^{125}I -photoreactive insulin in coated pits also occurred during the association period at 15°C (data not shown). When the cells were UV irradiated and further incubated for various periods at 37°C, the percentage of grains associated with the plasma membrane first dropped to reach minimal values by 30 to 60 min of incubation. Thereafter, within 5 h, their percentage progressively increased (Figs. 4 and 6B and Fig. 4 in reference 15).

When monensin (10^{-6} M) was added to the incubation medium, internalization of the labeled material was not impaired, but the subsequent recycling process was inhibited (Fig. 4). In contrast, cycloheximide (10^{-4} M) had no influence

² Data presented in Figs. 4 and 6B of the present paper and in Fig. 4 of reference 15 indicate that at the end of 2 h of incubation at 15°C, 85 and 82% of the radioactivity are associated with the plasma membrane. Taking into account a background of 10% it can be calculated that in the two cases the percent labeled material internalized represents 5 and 8%, respectively.

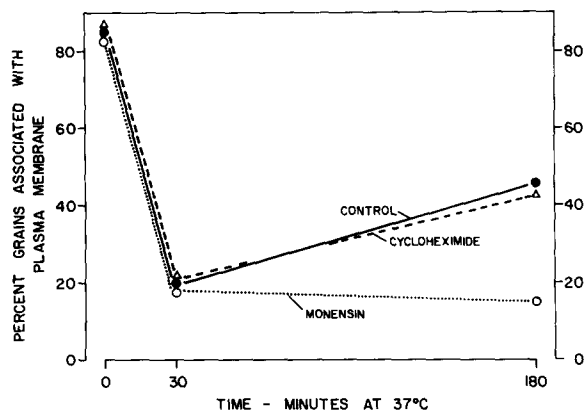


Figure 4. Relationship of autoradiographic grains with the plasma membrane of isolated hepatocytes. Cells were first incubated in the dark with ^{125}I -photoreactive insulin (45 ng/ml) for 2 h at 15°C. Hepatocytes were then UV irradiated, centrifuged, resuspended in insulin-free KRb buffer and incubated for various periods at 37°C. At each time point considered, cells were fixed with glutaraldehyde, 2.5% in cacodylate buffer (0.1 M, pH 7.4) and processed for quantitative EM autoradiography. Autoradiographic grains were considered to be associated with the plasma membrane if their center was <250 nm from the plasma membrane. When the influence of monensin (10^{-6} M) or cycloheximide (10^{-4} M) was tested, the drug was present in the incubation medium throughout the 37°C incubation.

on either the internalization or the recycling of ^{125}I -photoreactive insulin–receptor complexes, suggesting that at least up to 3 h of incubation, these processes are independent of protein synthesis (Fig. 4).

Quantitative Localization of ^{125}I -Photoreactive Insulin Inside the Hepatocytes

In the present study we have attempted to use the hypothetical grain method to obtain grain resolution. In this method grains are assigned to a given structure by a probability circle (i.e., real grains) and expressed in terms of the distribution of grains from a random source (hypothetical grains). As previously shown (13), the ratio of grains/grid points expresses the probability that a given structure represents the source of cell associated radioactivity under any given circumstance. To improve the resolution of the technique by decreasing the number of structures considered, specialized plasma membrane regions were not separately analyzed in the present study. When intracellular structures were studied, two distinct compartments were preferentially labeled at all time points. These included clear vesicles and lysosome-like structures (Fig. 5). The lysosome-like structures can be subdivided into multivesicular bodies and more typical lysosomes (i.e. dense bodies, glycogenosomes, etc.) (Fig. 5). Other intracellular compartments analyzed (i.e., mitochondria, endoplasmic reticulum, glycogen, Golgi complex, or cytoplasmic matrix [cytosol]) showed little, if any, labeling.

Distribution of Cell-associated Radioactivity as a Function of Incubation Time

Until this point of the study we used the hypothetical grain method of analysis to define those cellular structures that contain the source of the cell-associated radioactivity. To determine whether the proportion of radioactivity contained in these intracellular compartments changed as a function of

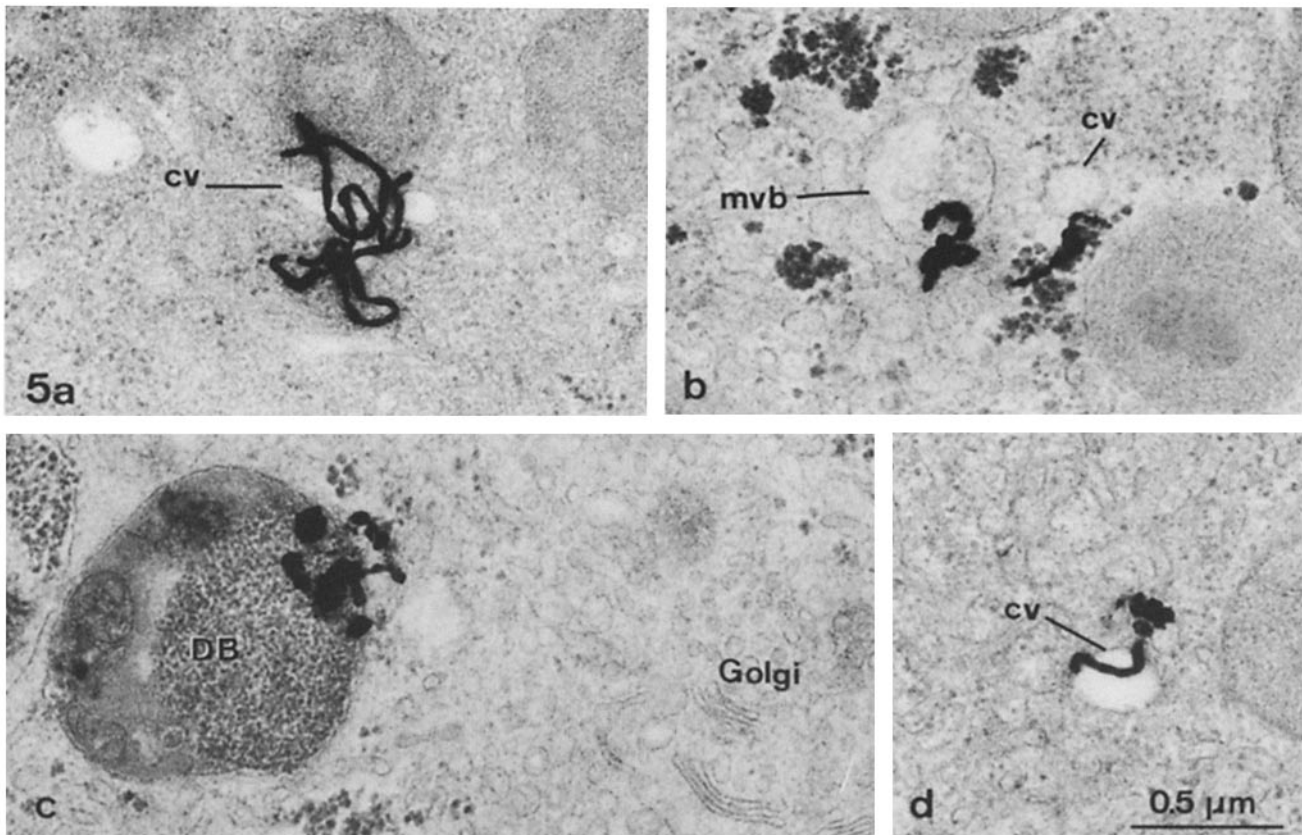


Figure 5. Representative examples of intracellular structures with which a preferential association of the labeled material was observed. The hepatocytes were incubated for 2 h at 15°C with ¹²⁵I-photoreactive insulin, UV irradiated, washed, and further incubated in the absence of labeled ligand for 0 min (a and b), 30 min (c), or 300 min (d) at 37°C. cv, clear vesicles; mvb, multivesicular body; DB, dense body.

Table I. Volume Densities of Clear Vesicles (CV), Multivesicular Bodies (MVB), and Dense Bodies in Freshly Isolated Hepatocytes at the Beginning and the End of the Incubation at 37°C

Time at 37°C (min)	Volume density of organelles × 10 ²	
	0	300
CV	262.4 ± 35.2 n = 43	232.5 ± 24.8 n = 48
MVB	117.2 ± 32.8 n = 43	88.4 ± 20.8 n = 48
Dense bodies	461.1 ± 74.1 n = 43	478.7 ± 78.2 n = 48

incubation time we evaluated the percentage of grains associated with these labeled compartments at the different incubation times at 37°C (see Materials and Methods). These values are representative of the labeling changes inside these compartments since the relative cytoplasmic volumes occupied by these structures remained practically unchanged with incubation time (Table I). After a 2-h incubation of isolated hepatocytes in the presence of ¹²⁵I-photoreactive insulin at 15°C, >40% of the autoradiographic grains found inside the cell were associated with clear vesicles, whereas only 10–15% were associated with lysosome-like structures (Fig. 6A). With increasing incubation time at 37°C, labeling of clear vesicles diminished until 90 min, when it reached a minimum. Thereafter, the labeling of clear vesicles increased slightly in a manner parallel to the reappearance of ¹²⁵I-photoreactive

insulin-receptor complexes on the cell surface (Fig. 6, A and B). A labeling pattern mirroring this process was observed for lysosome-like structures (Fig. 6A).

For the above analysis, multivesicular bodies were included in the lysosome-like compartment. To understand better their role in the internalization-recycling process, their labeling was analyzed in terms of the lysosome-like compartment at the various time points studied. As shown in Fig. 7, the percentage of multivesicular bodies among the population of lysosome-like structures was the highest by 30 min of incubation of freshly isolated rat hepatocytes at 37°C. Later on their proportion rapidly decreased and was maintained at the minimum value for up to 5 h (Fig. 7). These data suggest that multivesicular bodies are involved in the internalization process as prelysosomal structures and that they do not seem to play a role in the recycling process. We wished to determine next if the clear vesicles identified during the first 60 min of incubation at 37°C could be distinguished from those found after longer incubations. We measured the mean diameter of these vesicles in both conditions and found that their mean size and range of values were superposable (Fig. 8). In addition, the mean size of clear vesicles (210.6 nm and 215.4 nm) was less than half that of multivesicular bodies (≈580 nm).

When incubations were carried out in the presence of monensin (10⁻⁶ M) for up to 30 min of incubation, the sequence of events was similar to that described in control conditions (Fig. 9). After longer incubations, the monensin-treated cells behaved differently from control cells since the labeling of clear vesicles continued to decrease to reach values

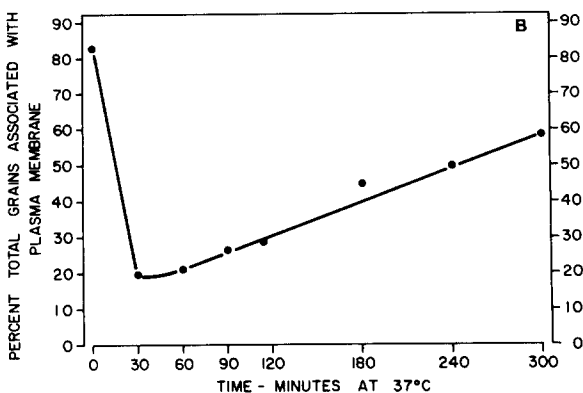
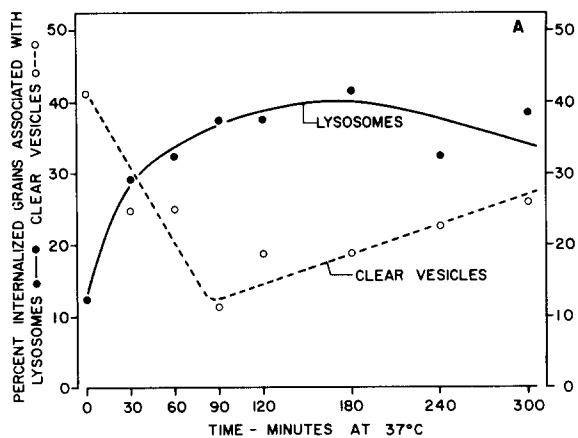


Figure 6. (A) Percentage of the total number of grains found inside freshly isolated rat hepatocytes that are associated with clear vesicles and lysosome-like structures as a function of incubation time at 37°C. Hepatocytes (0.5×10^6 per ml) were first incubated in the dark with ^{125}I -photoreactive insulin (45 ng/ml) for 2 h at 15°C. Cells were then UV irradiated, centrifuged, resuspended in insulin-free KRb buffer, incubated for various periods at 37°C, fixed, and processed for quantitative EM autoradiography. Autoradiographic grains were considered to be (specifically) associated with these structures if the grains were <250 nm away from the particular structure. If a clear vesicle and a lysosome were both within 250 nm of the center of the grain, the source of radioactivity responsible for this grain was considered to have a 50% chance of being associated with each of the two structures. (B) Percentage of the total number of grains associated with freshly isolated rat hepatocytes that are found within 250 nm from the plasma membrane. The experiment is the same as that analyzed in A; and these results are derived from reference 15.

close to zero, whereas labeling of lysosome-like structures increased (Fig. 9). In these conditions most lysosome-like structures were dilated multivesicular bodies (Fig. 2).

Discussion

Based on the data presented, we can conclude that the ^{125}I -photoreactive insulin-receptor complexes are internalized by an adsorptive endocytotic process involving the same structures as those described in the course of ^{125}I -insulin internalization, i.e., coated pits, coated vesicles, clear vesicles (endosomes), multivesicular bodies, and finally more typical lysosomes. Later, by the time the internalized but undegraded

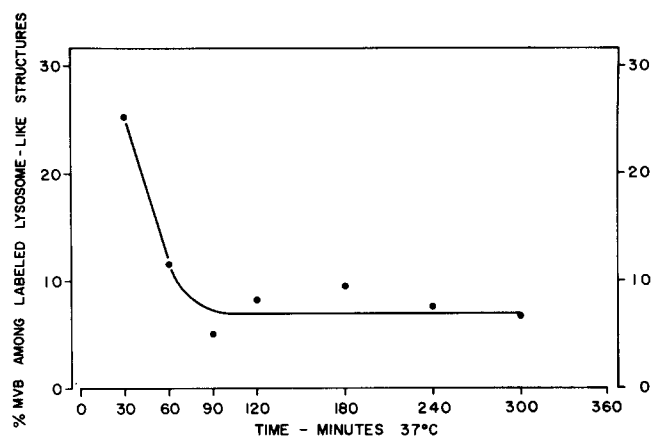


Figure 7. Percentage of the total number of lysosome-like structures that have morphological characteristics of multivesicular bodies (MVB); electron lucent content with small vesicles, presence of plaque with a coat attached to the cytoplasmic leaflet of the limiting membrane. This quantification was carried out in freshly isolated rat hepatocytes incubated as described in Fig. 4.

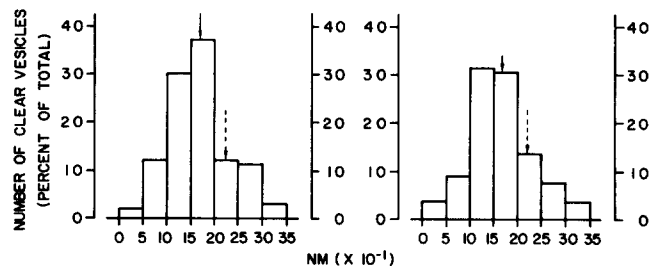


Figure 8. Size distribution histogram of clear vesicles involved in the internalization (0- to 60-min incubation at 37°C) (left) and in the recycling (180- to 360-min incubation at 37°C) (right) of ^{125}I -photoreactive insulin receptor complexes in freshly isolated rat hepatocytes. The percentage of clear vesicles is plotted as a function of their diameter. The solid arrows indicate the calculated mean diameter (left: $169.6 \text{ nm} \pm 5.7$, $n = 107$; right: $165.9 \text{ nm} \pm 6.6$, $n = 84$), and the broken arrows indicate the mean diameter corrected according to Weibel (45) (left: 215.4 nm ; right: 210.6 nm).

^{125}I -photoreactive insulin-receptor complexes recycle back to the cell surface, their association with clear vesicles progressively increases.

These data suggest a shuttling of insulin receptor between the plasma membrane and lysosome-like structures via a vesicular compartment. These observations may appear contradictory, with numerous recent studies suggesting that specific prelysosomal structures participate in the uncoupling of the ligand and its specific receptor and represent sorting centers from which a lysosomal destination is reserved for the ligands, whereas membrane bound receptors are directed mostly towards the cell surface (for review see references 5, 30, and 40). This distinction is, however, far from absolute since direct experimental evidence for the recycling of the interiorized plasma membrane by way of the lysosomes was provided by Muller et al. (28, 29) and Schneider et al. (32, 33). Thus membrane recycling via lysosomes can occur. The endosomal, and lysosomal pathways of recycling may not be mutually exclusive but may be quantitatively different under different experimental conditions.

In the case of insulin receptors the physiological relevance

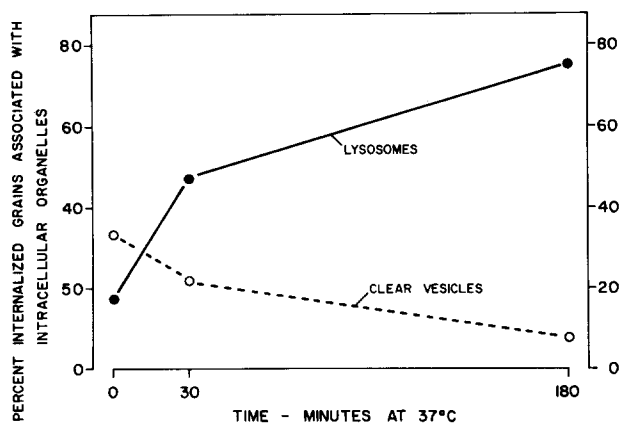


Figure 9. Percentage of the total number of grains found inside hepatocytes that are associated with clear vesicles and lysosome-like structures as a function of incubation at 37°C in the presence of monensin (10^{-6} M). Incubation conditions are identical to those described in Fig. 3. Autoradiographic grains found within 250 nm of one of the two intracellular compartments were considered to be associated with that compartment. If a clear vesicle and a lysosome-like structure were both within 250 nm of the center of a grain, the source of radioactivity responsible for the production of this grain was considered to have a 50% chance of being associated with each of these two structures.

of the recycling process occurring at a slow rate through the lysosomal pathway is, however, puzzling. Hepatocytes, indeed, rapidly internalize insulin receptors without simultaneously decreasing the number of their cell surface insulin receptors to a large extent (3; Gazzano, H., and E. Van Obberghen, unpublished observation). On the other hand, in a recent study we have shown that cells with a rapid internalization rate have an associated active recycling process designed to maintain at a constant level the number of cell surface insulin receptors (7). Based on these observations we would expect to find hepatocytes equipped with a rapid insulin receptor recycling process. The lysosomal pathway of recycling described in the present paper clearly does not satisfy these conditions. These discrepancies between our expectations and our experimental findings could be related to the experimental set up used in the present work, in which an irreversible binding of the ligand to its receptor occurs; this could affect insulin receptor recycling either by slowing down the normal route usually followed by the receptor or by bypassing another pathway of the receptor. Recently, Mellman et al. noted that the interaction of Fc receptors with polyvalent immune complexes leads to the delivery of receptors to lysosomes in contrast to the interaction with monovalent ligand which results in recycling through endosomes (26, 27). Based on these data the authors propose that the state of receptor aggregation in endosome membranes determines the fate of the receptors. By analogy with these studies, one could similarly speculate that the undissociability of photoreactive insulin impairs the disaggregation of receptor clusters in a prelysosomal compartment and prevents the inclusion of free receptors into nascent recycling vesicles (26). Under these conditions the insulin receptor complexes would be preferentially routed to lysosomes from which they retain the ability to recycle but at slower rate than from endosomes. Supporting this concept is the observation that the proportion of internalized plasma membrane recycling by way of lyso-

somes may be no more than 3% of the total, and that it occurs at a slow rate (6). We, therefore, favor the idea that the covalent linking of ^{125}I -photoreactive insulin to its receptor results in the bypassing of one of the recycling pathways (the endosomal one) and in the identification of a second recycling route involving lysosomes.

Lysosomotropic agents—better renamed acidotropic according to de Duve (12)—such as primary amines, chloroquine, monensin, etc., have been shown to interfere with receptor recycling (2, 11, 20, 41, 42). The rise in endolysosomal pH caused by these drugs that leads to a decreased dissociability of the ligand is frequently cited to explain their inhibitory effect on endosomal sorting and recycling process. Present data support this concept since the nondissociability of ^{125}I -photoreactive insulin from its receptor apparently impairs the sorting and recycling from the endosomal compartment. In contrast, the dissociability of the ligand does not seem to be a prerequisite for transport to lysosomes since in our system the photoreactive insulin receptor complexes are routed to this compartment. Beside its direct effect on endolysosomal pH, monensin could, like NH_4Cl , exert additional effects such as vacuolization, which may be the result of osmotic forces (14, 34, 45). This extensive vacuolization could result from (or in) an incapacity of treated cells to form recycling vesicles, leading to an accumulation inside the cell of the pool of recycling membrane (14, 40). This inhibitory effect would explain the lack of recycling by way of lysosomes observed in the present study under the influence of monensin.

Another point of interest from the study concerns the identification of the structures involved in the recycling of insulin receptors via the lysosomal pathway. In contrast to what was proposed for transferrin receptors (22), we did not find any evidence for the involvement of multivesicular bodies or Golgi cisternae in the return of insulin receptor back to the cell surface; instead, clear vesicles, which can have an elongated shape, were shown to be responsible for this transport. These vesicles are of similar size, shape, and electron density as vesicles involved in the internalization process. Whether these recycling vesicles contain lysosomal enzymes or not remains an open question.

We are indebted to G. Berthet and N. Dupont for skilled technical and typographical assistance. We thank Dr. D. Brandenburg, Wolforschung Institute, Aachen, Federal Republic of Germany, for providing photoreactive insulin, and Dr. P. Gorden, NIADDK, NIH, Bethesda, MD, for critical reading of the manuscript. This investigation was supported by grant. 3.460.83 from the Swiss National Science Foundation.

Received for publication 10 October 1985, and in revised form 25 November 1985.

References

- Anderson, R. G. W., J. L. Goldstein, and M. S. Brown. 1977. A mutation that impairs the ability of lipoprotein receptors to localize in coated pits on the cell surface of human fibroblasts. *Nature (Lond.)* 270:695-699.
- Basu, S. K., J. L. Goldstein, R. G. W. Anderson, and M. S. Brown. 1981. Monensin interrupts the recycling of low density lipoprotein receptors in human fibroblasts. *Cell*. 24:493-502.
- Blackard, W. G., P. S. Guzelian, and M. E. Small. 1978. Down regulation of insulin receptors in primary cultures of adult rat hepatocytes in monolayer. *Endocrinology*. 103:548-551.
- Blackett, N. M., and D. M. Parry. 1977. A simplified method of "hypothetical grain" analysis of electron microscope autoradiographs. *J. Histochem. Cytochem.* 25:206-214.

5. Brown, M. S., R. G. W. Anderson, and J. L. Goldstein. 1983. Recycling receptors: the round-trip itinerary of migrant membrane proteins. *Cell* 32:663-667.
6. Burgert, H. G., and L. Thilo. 1983. Internalization and recycling of plasma membrane glycoconjugates during pinocytosis in the macrophage cell line P 388 D₁. *Exp. Cell Res.* 144:127-142.
7. Carpentier, J.-L., J.-M. Dayer, U. Lang, R. Silverman, P. Gorden, and L. Orci. 1984. Down regulation and recycling of insulin receptors: effect of monensin on IM-9 lymphocytes and U-937 monocyte-like cells. *J. Biol. Chem.* 259:14190-14195.
8. Carpentier, J.-L., M. Fehlmann, E. Van Obberghen, P. Gorden, and L. Orci. 1985. Redistribution of ¹²⁵I-insulin on the surface of rat hepatocytes as a function of dissociation time. *Diabetes* 34:1002-1007.
9. Carpentier, J.-L., P. Gorden, M. Amherdt, E. Van Obberghen, C. R. Kahn, and L. Orci. 1978. ¹²⁵I-insulin binding to cultured human lymphocytes: initial localization and fate of hormone determined by quantitative electron microscopic autoradiography. *J. Clin. Invest.* 61:1057-1070.
10. Carpentier, J.-L., P. Gorden, P. Freychet, A. Le Cam, and L. Orci. 1979. Lysosomal association of internalized ¹²⁵I-insulin in isolated rat hepatocytes: direct demonstration by quantitative electron microscopic autoradiography. *J. Clin. Invest.* 63:1249-1261.
11. Ciechanover, A., A. L. Schwartz, A. Dautry-Varsat, and H. F. Lodish. 1983. Kinetics of internalization and recycling of transferrin and the transferrin receptor in a human hepatoma cell line. *J. Biol. Chem.* 258:9681-9689.
12. de Duve. 1983. Lysosomes revisited. *Eur. J. Biochem.* 137:391-397.
13. Fan, J. Y., J.-L. Carpentier, E. Van Obberghen, N. M. Blackett, C. Grunfeld, P. Gorden, and L. Orci. 1983. The interaction of ¹²⁵I-insulin with cultured 3T3-L1 adipocytes: quantitative analysis by the hypothetical grain method. *J. Histochem. Cytochem.* 31:859-870.
14. Fedorko, M. E., J. G. Hirsch, and Z. A. Cohn. 1968. Autophagic vacuoles produced in vitro. I. Studies on cultured macrophages exposed to chloroquine. *J. Cell Biol.* 38:377-391.
15. Fehlmann, M., J.-L. Carpentier, E. Van Obberghen, P. Freychet, P. Thamm, D. Saunders, D. Brandenburg, and L. Orci. 1982. Internalized insulin receptors are recycled to the cell surface in rat hepatocytes. *Proc. Natl. Acad. Sci. USA* 79:5921-5925.
16. Fehlmann, M., J.-L. Carpentier, A. Le Cam, P. Thamm, D. Saunders, D. Brandenburg, L. Orci, and P. Freychet. 1982. Biochemical and morphological evidence that the insulin receptor is internalized with insulin in hepatocytes. *J. Cell Biol.* 93:82-87.
17. Fehlmann, M., Le Marchand-Brustel, Y., Van Obberghen, E., Brandenburg, D., Freychet, P. 1982. Photoaffinity labelling of the insulin receptor in intact rat hepatocytes, mouse soleus muscle and cultured human lymphocytes. *Diabetologia* 23:440-444.
18. Freychet, P. 1976. Insulin receptors. In *Methods in Receptor Research*, Part II. M. Blecher, editor. Marcel Dekker Inc., New York. 385-428.
19. Geuze, H. J., J. W. Slot, G. J. A. M. Strous, H. F. Lodish, and A. L. Schwartz. 1983. Intracellular site of asialoglycoproteins receptor-ligand uncoupling: double-label immunoelectron microscopy during receptor-mediated endocytosis. *Cell* 32:277-287.
20. Gonzales-Noriega, A., J. H. Grubb, V. Talkad, and W. S. Sly. 1980. Chloroquine inhibits lysosomal enzymes pinocytosis and enhances lysosomal enzyme secretion by impairing receptor recycling. *J. Cell Biol.* 85:839-852.
21. Gorden, P., J.-L. Carpentier, M. L. Moule, C. C. Yip, and L. Orci. 1982. Direct demonstration of insulin receptor internalization: a quantitative electron microscopic study of covalently bound ¹²⁵I-photoreactive insulin incubated with isolated hepatocytes. *Diabetes* 31:659-662.
22. Harding, C., J. Heuser, and P. Stahl. 1983. Receptor-mediated endocytosis of transferrin and recycling of the transferrin receptor in rat reticulocytes. *J. Cell Biol.* 97:329-339.
23. Helenius, A., I. Mellman, D. Wall, and A. Hubbard. 1983. Endosomes. *Trends Biochem. Sci.* 8:245-250.
24. Kaplan, J. 1980. Evidence for reutilization of surface receptors for α_2 -macroglobulin protease complexes in rabbit alveolar macrophages. *Cell* 19:197-205.
25. Karin, M., and B. Mintz. 1981. Receptor-mediated endocytosis of transferrin in developmentally totipotent mouse teratocarcinoma stem cells. *J. Biol. Chem.* 256:3245-3252.
26. Mellman, I., and M. Plutner. 1984. Internalization and degradation of macrophage Fc receptors bound to polyvalent immune complexes. *J. Cell Biol.* 98:1170-1177.
27. Mellman, I., H. Plutner, and P. Ukkonen. 1984. Internalization and rapid recycling of macrophage Fc receptors tagged with monovalent antireceptor antibody: possible role of a prelysosomal compartment. *J. Cell Biol.* 98:1163-1169.
28. Muller, W. A., R. M. Steinman, and Z. A. Cohn. 1980. The membrane proteins of the vacuolar system. II. Bidirectional flow between secondary lysosomes and plasma membrane. *J. Cell Biol.* 86:304-314.
29. Muller, W. A., R. M. Steinman, and Z. A. Cohn. 1983. Membrane proteins of the vacuolar system. III. Further studies on the composition and recycling of endocytotic vacuole membrane in cultured macrophages. *J. Cell Biol.* 96:29-36.
30. Pastan, I. M., and M. C. Willingham. 1981. Journey to the center of the cell: role of the receptosome. *Science (Wash. DC)* 214:504-509.
31. Salpeter, M. M., H. C. Fertuck, and E. E. Salpeter. 1977. Resolution in electron microscope autoradiography. III. Iodine-125. The effect of heavy metal staining and a reassessment of critical parameters. *J. Cell Biol.* 72:161-173.
32. Schneider, Y.-J., C. de Duve, and A. Trouet. 1981. Fate of plasma membrane during endocytosis. III. Evidence for incomplete breakdown of immunoglobulins in lysosomes of cultured fibroblasts. *J. Cell Biol.* 88:380-387.
33. Schneider, Y.-J., P. Tulkens, C. de Duve, and A. Trouet. 1979. Fate of plasma membrane during endocytosis. II. Evidence for recycling (shuttle) of plasma membrane constituents. *J. Cell Biol.* 82:466-474.
34. Schwartz, A. L., A. Bolognesi, and S. E. Fridovich. 1984. Recycling of the asialoglycoprotein receptor and the effect of lysosomotropic amines in hepatoma cells. *J. Cell Biol.* 98:732-738.
35. Schwartz, A. L., S. E. Fridovich, and M. F. Lodish. 1982. Kinetics of internalization and recycling of the asialoglycoprotein receptor in a hepatoma cell line. *J. Biol. Chem.* 257:4230-4237.
36. Seglen, P. O. 1976. Preparation of isolated rat liver cells. *Methods Cell Biol.* 13:29-83.
37. Stahl, P., P. H. Schlesinger, E. Sigardson, J. S. Rodman, and Y. C. Lee. 1980. Receptor-mediated pinocytosis of mannose glycoconjugates by macrophages: characterization and evidence for receptor recycling. *Cell* 19:207-215.
38. Steer, C. J., and G. Ashwell. 1980. Studies on a mammalian hepatic binding protein specific for asialoglycoprotein: evidence for receptor recycling in isolated rat hepatocytes. *J. Biol. Chem.* 255:3008-3013.
39. Steinman, R. M., S. E. Brodie, and Z. A. Cohn. 1976. Membrane flow during pinocytosis: a stereologic analysis. *J. Cell Biol.* 68:665-687.
40. Steinman, R. M., I. S. Mellman, W. A. Muller, and Z. A. Cohn. 1983. Endocytosis and the recycling of plasma membrane. *J. Cell Biol.* 96:1-27.
41. Tolleshaug, H., and T. Berg. 1979. Chloroquine reduces the number of asialoglycoprotein receptors in the hepatocyte plasma membrane. *Biochem. Pharmacol.* 28:2912-2922.
42. van Leuven, F., J.-J. Cassiman, and H. van den Berghe. 1980. Primary amines inhibit recycling of α_2 M receptors in fibroblasts. *Cell* 20:37-43.
43. Tycko, B., and F. R. Maxfield. 1982. Rapid acidification of endocytic vesicles containing α_2 -macroglobulin. *Cell* 28:643-651.
44. Weibel, E. R. 1969. Stereological principles for morphometry in electron microscope cytology. *Int. Rev. Cytol.* 26:235-302.
45. Wilcox, D. K., R. P. Kitson, and C. C. Widnell. 1982. Inhibition of pinocytosis in rat embryo fibroblasts treated with monensin. *J. Cell Biol.* 92:859-864.
46. Zigmund, S. H., S. J. Sullivan, and D. A. Lauffenburger. 1982. Kinetic analysis of chemotactic peptide receptor modulation. *J. Cell Biol.* 92:34-43.